Desalination and Water Treatment
www.deswater.com
doi: 10.5004/dwt.2020.25952

197 (2020) 335–344
September

Decolourization of aqueous Methylene Blue solutions by corn stalk: modeling and optimization

Seyyed Alireza Mousavi[a,b,*], Hadis Zangeneh[a], Ali Almasi[a,b], Danial Nayeri[a,c], Mahya Monkaresi[a], Arezoo Mahmoudi[a], Parastoo Darvishi[a]

[a]*Department of Environmental Health Engineering, School of Public Health, Research Center for Environmental Determinants of Health (RCEDH), Kermanshah University of Medical Sciences, Kermanshah, Iran, emails: seyyedarm@yahoo.com/ sar.mousavi@kums.ac.ir (S.A. Mousavi), hadiszangene@yahoo.com (H. Zangeneh), alialmasi@yahoo.com (A. Almasi), nayeri.danyal1997@gmail.com (D. Nayeri), m.monkaresi@gmail.com (M. Monkaresi), aam.740428@gmail.com (A. Mahmoudi), Pd.740531@gmail.com (P. Darvishi)*
[b]*Social Development and Health Promotion Research Center, Kermanshah University of Medical Sciences, Kermanshah, Iran*
[c]*Student's research committee, Kermanshah University of Medical Sciences, Kermanshah, Iran*

Received 8 January 2019; Accepted 12 April 2020

ABSTRACT

The aim of the current study was to synthesis activated carbon from corn stalk using a simple thermal activation method. The physical and chemical characteristics of prepared activated carbon have been investigated using scanning electron microscopy, Brunauer–Emmett–Teller, Fourier-transform infrared spectroscopy, and pH of zero point charge (pH_{ZPC}). Then, the application of the prepared corn stalk activated carbon was investigated to remove the Methylene Blue (MB) dye from aqueous solution. The effect of four independent factors including initial concentration (10–210 mg L^{-1}), adsorbent dosage (0.2–1.4 g L^{-1}), pH (3–11), and contact time (10–50) were also evaluated by response surface methodology at five levels. Complete dye removal was observed at an initial concentration of 10 mg L^{-1}, and adsorbent dosage of 1.4 g, pH of 11, and contact time of 50 min. The adsorption kinetics was also described by the pseudo-second-order model with R^2 = 0. 9833. The results of comparison equilibrium data between Langmuir and Freundlich models showed that the adsorption process was best described by Freundlich with the maximum adsorption capacity q_m = 2.34 mg g^{-1}. The experimental data were also fitted with Freundlich isotherm (R^2 = 0.91). Base on the results, it can be concluded that corn stalk activated carbon produced from agricultural wastes is a highly promising nontoxic and environmentally friendly adsorbent with great potential for removing of MB.

Keywords: Activated carbon; Corn stalk; Methylene Blue; Central composite design; Modeling and optimization; Kinetic analysis

1. Introduction

Recently, the world is experiencing freshwater scarcity due to the growing increase of global economic, population, and unplanned urbanization [1]. Besides, the rapid advances in different industries have led to produce high quantities of wastewater from industrial processes, finally release different pollutants such as nitrogen components [2,3], organic carbon [4], heavy metals [5], and dyes [6] into water resources without meeting requirements. These wastewaters usually contain recalcitrant contaminations, which have different resistance to biological degradation in water and soil [6].

The dyes are important pollutants in wastewaters, which are mainly discharged from industries like textile, printing, food, and leather, etc [7,8]. The colored wastewaters

* Corresponding author.

possess different kinds of dyes that most of them are considered to be non-oxidizable owing to their large sizes and complicated molecular structure [6]. Various techniques such as coagulation [9,10], flocculation [9,10], nano photocatalyst [11–13], membrane filtration [14], nano-sorbents [15], or biosorbents [16] have been applied for the removal of these pollutants from aqueous medium. Many of these methods suffer drawbacks of simply transferring the pollutant from one phase to another, large energy requirements (e.g., thermal destruction), and requiring long treatment periods (e.g., biological treatment) [8]. Recently, the adsorption process has been established as a valuable technique for dye removal. Adsorption is one of the best solutions for the removal of dyes from the wastewater due to its cost-effective nature [15,17], low development cost, simple design, free from toxic substances, easy, and safe recovery of adsorbent [15,16], high efficiency, simplicity, high selectivity at the molecular level, low energy consumption, ability to separate numerous chemical compound, design flexibility, technological maturity, ability to regenerate the used adsorbent, high reliability and easy operation [16–18]. Although adsorption is a widely used method for dye removal but resulted in secondary pollution [16]. Among different adsorbent materials, activated carbon has received much attention due to its high adsorption efficiency and high surface area [19].

Recently, many efforts have been done to produce low cost activated carbon from agricultural waste due to its availability in large quantities and high carbon content [20]. The corn stalk has great potential to produce activated carbon due to availability, biodegradability, nontoxic properties, low cost [21,22]. Cornstalk composed of cortex and core. The cortex is composed of cellulose and lignin [23]. The cellulose content has a high hydroxyl group resulting in high adsorption capacity. It has been estimated that about 520 × 109 kg of corn stalk is produced annually in the world [24]. Some investigations are done to remove Methylene Blue (MB) with adsorbents which are produced from breadnut peel [25], cotton stalk [26], wood apple shell (*Feronia acidissima*) [27], canola residues [28], *Ageratum conyzoides* leaf powder [29].

In this work, corn stalk activated carbon was synthesized, characterized, and applied to the adsorption of MB as a cationic dye. The effect of initial dye concentration, adsorbent dosage, pH, and contact time on the adsorption efficiency was also evaluated. The adsorption experiments were also modeled and optimized using a central composite design (CCD). The adsorption isotherm equation was used to investigate equilibrium data. The kinetic of MB adsorption was studied at optimum operating conditions.

2. Material and methods

2.1. Chemicals and reagents

In this study, MB with high purity (99.9%) and all chemicals were analytical grades and purchased from (Merck, Germany). HCl (0.1 M) and NaOH (0.1 M) used for adjusting the pH using pH meter (WTW, Germany).

2.2. Synthesis of corn stalk activated carbon

The corn stalk was collected from the farm located in Kermanshah, Iran, and washed with deionized water several times to remove any impurities and then dried under sunlight after 8 h. The dried corn stalks were cut into pieces with an average size of 2–3 cm and then were milled to get small pieces (sieve with 50 mesh). The corn stalk pieces are separated with a mesh size of 40 and 28. After that, the small pieces were taken at a hot air oven (Germany, Memmert 854) about 4 h at 150°C. The activation was done in a furnace (Germany, Nabertherm 11/s27) at 500°C for 1 h under 150 mL min^{-1} N_2 flow. The cooled sample was then washed with HCl (0.1 M) at 110°C in a hydrothermal reactor for 1 h. The prepared powdered activated carbon (PAC) washed with deionized water to remove any impurities. Finally, the washed activated carbon was dried in a vacuum oven at 105°C overnight.

2.3. Characterization of the prepared activated carbon

Morphology of the prepared activated carbon was investigated by scanning electron microscopy (SEM) (MIRA III, Japan). Fourier-transform infrared spectroscopy (FTIR) spectra were recorded in KBr wafers with Alpha, Bruker FTIR (Germany). Brunauer–Emmett–Teller (BET) was measured using a BELSORP-mini II, Japan. Also, the pH of the zero point charge (pH_{ZPC}) was measured by the pH drift method [30].

2.4. Adsorption experiments

MB adsorption experiments were performed based on designed conditions using CCD as described in the following section. 100 mL of MB aqueous solution with the desired amount of adsorbent was added to 250 mL Erlenmeyer flasks which were placed on the incubator under stirring conditions at the rate of 200 rpm at 25°C. The samples were withdrawn at regular intervals. The samples were centrifuged (ShimiFan, Iran(at 4,000 rpm for 10 min. The centrifuged solution was analyzed by a UV-Vis spectrophotometer (Jenway 6305, Germany) at 675 nm then the efficiency of the system was calculated based on (Eq. (1)) [31]:

$$R(\%) = \frac{A_0 - A_t}{A_0} \times 100 \quad (1)$$

where A_0 and A_t are the initial and final concentration of MB after the adsorption process, respectively.

2.5. Experimental design

Response surface methodology (RSM) as a collection of the statistical and mathematical techniques was developed to process design, analysis, modeling, and optimization of experimental responses with least experimental when several variables influenced a response or a set of responses [4,5]. The results explore the optimal operating conditions using RSM. In this study, CCD based RSM was chosen for the optimization of four independent numerical variables (MB concentration, adsorbent dosage, pH, and contact time). The range of selected variables was determined using primarily tests as shown in Table 1. The experimental conditions and results also represented in Table 2. In this study, the results were completely analyzed using analysis of variance (ANOVA) automatically performed by Design-Expert software.

2.6. Kinetic study and equilibrium data

The adsorption kinetics was studied to determine the adsorption rate at MB concentration of 210 mg L^{-1}, pH of 7, different adsorbent concentration (0.2–1.4 g L^{-1}) at 200 rpm for different time intervals. This experiment continued until equilibrium conditions were reached when no further decrease in the MB concentration was measured.

The q_e and q_t were defined as the amount of MB adsorbed onto the corn stalk activated carbon at equilibrium and time t, respectively which could be illustrated as given Eqs. (2) and (3) [32]:

$$q_e\left(\frac{\text{mg}}{\text{g}}\right)=\frac{\left(C_0-C_e\right)\times V}{W} \tag{2}$$

$$q_t\left(\frac{\text{mg}}{\text{g}}\right)=\frac{\left(C_0-C_t\right)\times V}{W} \tag{3}$$

The kinetic of the MB adsorption process was studied using pseudo-first-order and pseudo-second-order models, respectively which are expressed by following Eqs. (4) and (5) [33]:

$$\log\left(q_e-q_t\right)=\log q_e-\frac{K_1}{2.303}t \tag{4}$$

$$\frac{t}{q_t}=\frac{1}{k_2q_e^2}+\frac{1}{q_e}t \tag{5}$$

To investigate the mechanism of MB adsorption, Langmuir, and Freundlich isotherm as an empirical model were also employed to correlate experimental adsorption data. The correlation coefficient (R^2) and standard errors were also evaluated to fit the best isotherm model.

The Langmuir isotherm model assumes that the adsorption process occurs on a finite number of definite sites and thickness of the adsorbed layer is one molecule or monolayer adsorption was formed on the adsorbent homogeneous sites [34]. The Freundlich isotherm model is often applied to describe the adsorption process on a heterogeneous surface. The Langmuir and Freundlich expressions are represented as Eqs. (6) and (7) [35]:

$$\frac{C_e}{q_e}=\frac{C_e}{q_m}+\frac{1}{q_m\times K_1} \tag{6}$$

$$\ln q_e=\ln k_f+\frac{1}{n}\ln C_e \tag{7}$$

Table 1
Independent variables and their levels for the design of the tests

Parameter name	Symbols	Low (–1)	High (+1)
Initial concentration, mg L^{-1}	*A*	10	210
Adsorbent dosage, g	*B*	0.2	1.4
pH	*C*	3	11
Contact time, min	*D*	10	50

Table 2
Experimental conditions and data for MB removal

Run	*A* (mg L^{-1})	*B* (g L^{-1})	*C*	*D* (min)	MB removal (%)
1	210	1.4	11	10	33.79
2	10	1.4	11	10	99.50
3	210	1.4	3	10	26.84
4	10	0.2	3	10	98.00
5	10	0.2	11	10	98.57
6	10	1.4	3	10	99.23
7	210	0.2	11	10	29.77
8	210	0.2	3	10	23.00
9	110	0.8	7	20	23.18
10	60	0.8	7	30	24.46
11	110	0.8	7	30	24.93
12	110	0.8	7	30	35.05
13	110	0.8	7	30	33.66
14	110	0.8	5	30	20.39
15	160	0.8	7	30	31.11
16	110	0.8	7	30	15.50
17	110	0.8	7	30	26.67
18	110	0.5	7	30	23.88
19	110	0.8	7	30	13.41
20	110	0.8	9	30	23.88
21	110	1.1	7	30	21.44
22	110	0.8	7	40	22.83
23	10	1.4	3	50	98.92
24	10	0.2	11	50	99.57
25	210	0.2	11	50	41.11
26	210	1.4	11	50	48.79
27	10	1.4	11	50	99.57
28	210	1.4	3	50	28.12
29	10	0.2	3	50	98.88
30	210	0.2	3	50	21.17

3. Results and discussion

3.1. Carbon characterization

SEM image of the prepared corn stalk activated carbon before the adsorption process is shown in Fig. 1a. The valleys or large pores, cracks, and crevices on the surface of activated carbon were observed which indicates its rough surface thereby increasing its porosity and improving the adsorption process. In Fig. 1b depicting the surfaces of particles after adsorption it is seen that the caves, pores, and surfaces of adsorbent were covered by MB dye molecules. As well, the surface area of the prepared activated carbon was estimated using BET analysis. Accordingly, the BET specific surface area of activated carbon prepared from corn stalk is 85.12 m^2 g^{-1}.

FTIR analysis was used to identify some characteristic functional groups of activated carbon before and after the dye adsorption as shown in Figs. 2a and b, respectively.

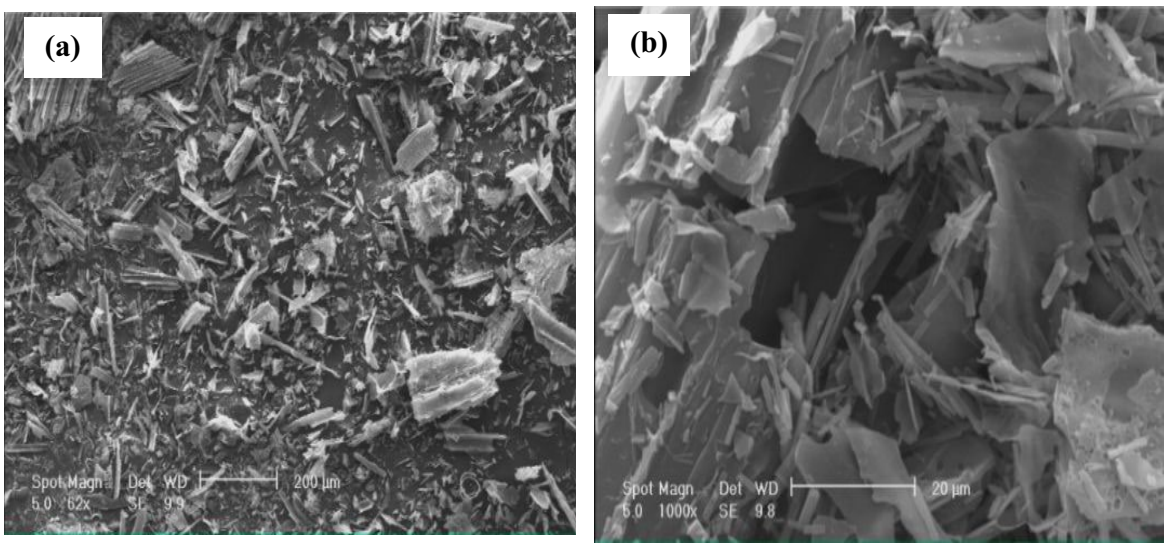

Fig. 1. SEM of activated carbon prepared from corn stalk (a) before and (b) after the adsorption process.

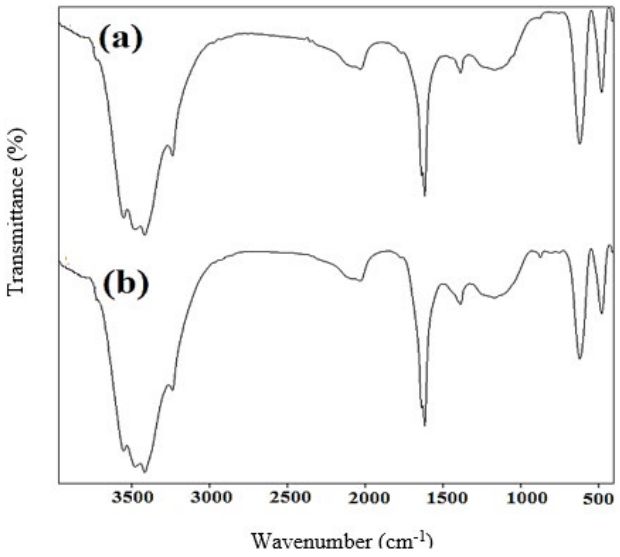

Fig. 2. FTIR spectrum of (a) activated carbon before MB adsorption and (b) regenerated activated carbon after MB adsorption.

The high intense band at 3,416 cm^{-1} corresponds to the O–H or N–H stretching vibrations thus indicating the presence of free hydroxyl or primary amine groups on the surface of adsorbent [31]. The bands at 1,600–1,700 cm^{-1} and 2,900–3,200 cm^{-1} are related to the stretching vibration of C=O and CH_2 groups [31,36]. In the region 1,400–1,600 cm^{-1}, there are clusters of complex bands, which may be due to the presence of aromatic (C=C) bands and various substitution modes of the aromatic rings [37]. The broadband at 1,387 and 1,168 cm^{-1} has been assigned to CH_3 bending vibration and C–C skeletal vibration [37]. Bands below 950 cm^{-1} correspond to the out-of-plane deformation vibrations of the C–H groups in the aromatic structure [36,37].

The MB adsorption process was done at MB concentration of 10 mg L^{-1}, 1.4 g L^{-1} of activated carbon and pH of 11 after 10 min. The activated carbon is centrifuged, washed with deionized water and dried at 110°C for about 3 h. Then the FTIR spectrum of regenerated activated carbon is recorded. The MB concentration is negligible after the regeneration process so, the FTIR spectrum of activated carbon was not changed after MB adsorption.

3.2. CCD process modeling and optimization

The ANOVA data is given in Table 3. As a result, the quadratic model was selected based on lower *p*-value (<0.001) and higher *F*-value (196.19) compared to the other suggested models and its expression was represented as follow:

$$\text{MB removal (\%)} = -26.16283 + 1.12537 \times A - 5.57285 \times B + 10.72673 \times C - 1.32135 \times D - 0.082652 \times A \times B - 0.014185 \times A \times C - 5.07437\text{E-}004 \times A \times D + 0.23115 \times B \times C + 0.051365 \times B \times D - 0.045919 \times C \times D - 1.00058\text{E-}003 \times A^2 + 2.03956 \times B^2 - 0.67411 \times C^2 + 0.026786 \times D^2 \quad (8)$$

Based on the *p*-value, parameters with a *p*-value higher than 0.05 are not significant. Therefore, *A*, *B*, *C*, *AB*, *AC*, and *CD* are significant and their degree of importance based on *F*-values are $A > C > AC > B > AB > CD$.

The *A* parameter (MB concentration) has a maximum effect on the response because dye concentration controls mass transfer resistance and the poisoning of adsorbent [38]. The R^2 value is about 0.9946, close to 1, indicates fully matched of proposed models with experimental data which is approved by the conformity of predicated and experimental data (Fig. 3). The high adequate precision (>4) and low coefficient of variation (C.V.) indicate high precision and good reliability of proposed models [38,39].

As can be seen in Table 3, MB adsorption (MB removal efficiency) affected by their parameters and interactions. Therefore, the three dimensional (3D) response surface plots were employed to evaluate their effects and achieve optimum conditions.

Two-dimensional response surface plot of pH and contact time as a function of the response at MB concentration of 110 mg L^{-1} and adsorbent dosage of 0.8 g L^{-1} are displayed in Fig. 4. As observed, the value of MB removal is low at pH of 3 up to 7 while its value increases up to 99.5% at a pH of 7 to 11. The alkaline pH shows a high MB adsorption capacity. The pH_{zpc} of the prepared activated carbon was determined using the pH drift method (Fig. 5). As observed, the pH of the zero charge point for activated carbon is about 5. It is indicated that the surface of activated carbon is positively charged at pH < 5 and its surface is negatively charged at pH > 5. At pH higher than the pKa of MB (3.8), MB molecules are positively charged. Therefore, at acidic pH, the repulsion attraction between MB molecules and activated carbon surface cause to decrease of MB adsorption. Also, with increasing pH of the solution, the number of hydroxyl groups increases which have a strong electrostatic attraction with positively charged MB molecules thereby improving adsorption capacity and color removal [39]. El Qada et al. [40] and Wang et al. [41] reported a similar result for MB adsorption. They observed that MB adsorption increases with an increase in pH of solution [40,41].

The effect of contact time on the response was also displayed in Figs. 4a and b. Dye removal was found to improve with increasing contact time. The adsorption rate was rapid at the initial period of contact time while it was slower with increasing contact time. Initially, the active sites of activated carbon are vacant and the MB concentration gradient is high. However, the sites of adsorbent

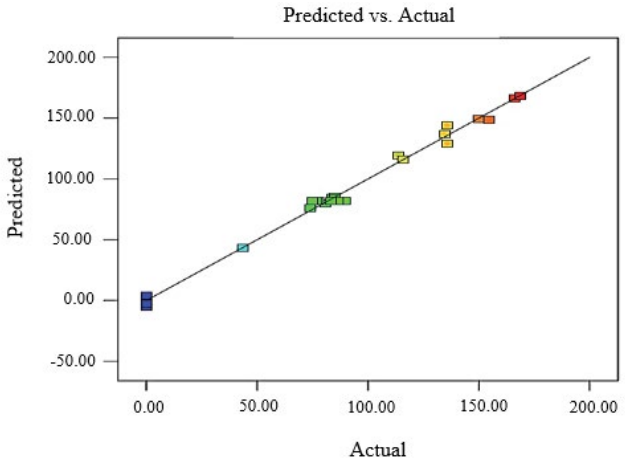

Fig. 3. Predicted vs. actual data.

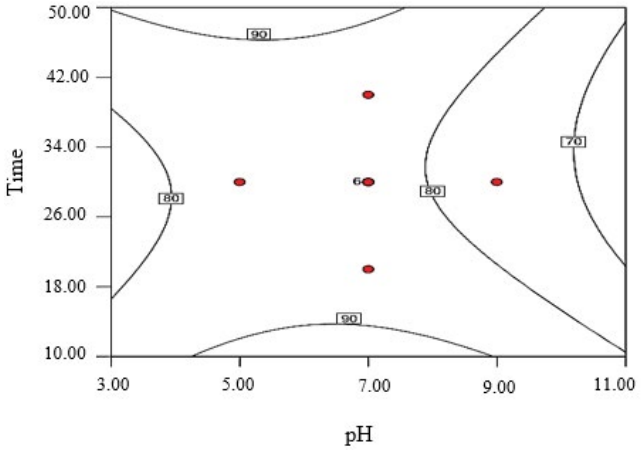

Fig. 4. Two-dimensional response surface plot correlation between initial pH and reaction time on MB removal at an initial concentration of 110 mg L^{-1} and adsorbent dosage of 0.8 g.

Table 3
Developed models and ANOVA results using Design Expert 7.0.0.1 for studied responses

Source	Coefficient estimate	Sum of squares	*df*	Mean square	*F*-value	*P*-value
Model	81.90	89,417.25	14	6,386.95	196.11	0.0001
A-*C*	72.46	86,633.32	1	86,633.32	2,661.13	0.0001
B-PAC	–4.95	403.54	1	403.54	12.40	0.0031
C-pH	–5.86	565.68	1	565.68	17.38	0.0008
D-Time	–1.01	16.74	1	16.74	0.51	0.4843
AB	–4.96	393.49	1	393.49	12.09	0.0034
AC	–5.67	515.11	1	515.11	15.82	0.0012
AD	–1.01	16.48	1	16.48	0.51	0.4877
BC	0.55	4.92	1	4.92	0.15	0.7028
BD	0.62	6.08	1	6.08	0.19	0.6718
CD	–3.67	215.91	1	215.91	6.63	0.0211
A^2	–10.01	16.66	1	16.66	0.51	0.4854
B^2	0.73	0.09	1	0.09	2.7 E-003	0.9588
C^2	10.79	19.36	1	19.36	0.59	0.4526
D^2	10.71	19.10	1	19.10	0.59	0.4555
Residual	–	488.33	15	32.56	–	–

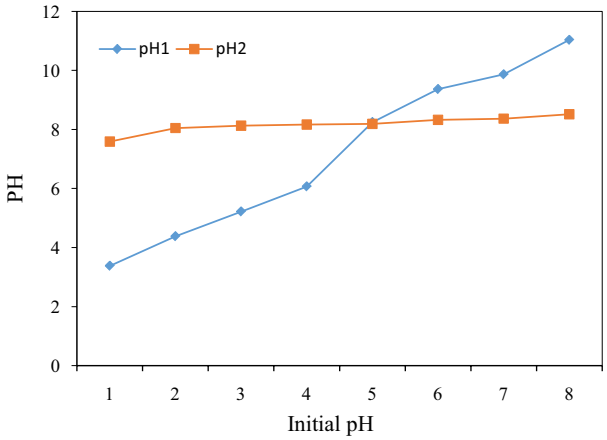

Fig. 5. pH_{zpc} of the prepared activated carbon using a pH drift method.

were saturated during the adsorption process thereby increasing the unavailability of active sites [42].

The effect of initial MB concentration and adsorbent dosage on the response at a contact time of 30 min and pH equal 7 was also illustrated as shown in three-dimensional (3D) and two-dimensional response surface plots (Figs. 6a and b), respectively. Dye removal efficiency reduced from 99.5% to 21% with varying MB concentrations from 10 up to 210 mg L^{-1}. The adsorbent dosage has a reveres effect. When the adsorbent dose changes from 0.2 to 1.4 g L^{-1}, dye removal improves about 75.5%. At low MB concentration, the ratio of surface active sites to dye molecules is high so the dye molecules can be employed the vacant sites on the adsorbent surface resulting enhancement of color removal. However, at a high concentration of MB, the active sites of adsorbent diminish thereby decreasing MB removal efficiency which agrees with the observation of Pirbazari et al. [8]. They found that increases in MB concentration from 20 to 50 mg L^{-1} cause to reduce adsorption capacity from 152 to 62.6 mg L^{-1} [8]. Mulugeta and Lelisa [43] was also reported a similar result in which adsorption rate reduces with changing MB concentration from 50 to 400 mg L^{-1} [43]. As activated carbon concentration increases MB removal improves due to the increasing number of reaction sites. A similar result was reported by Khairud Dahri et al. [44]. They observed that the various mass of adsorbent from 0.01 to 0.03 g increase MB removal from 57% to 91% [44].

3.3. Adsorption isotherms and kinetics

Langmuir and Freundlich isotherms for MB adsorption are given in Figs. 7a and b, respectively. The calculated Langmuir and Freundlich constants and R^2 values for both of the isotherm models are also given in Table 4. As can be seen, the R^2 of the Freundlich model (0.9139) is higher than its value for Langmuir isotherm (0.9032). This is suggested that the experimental data was more fitted with the Freundlich model. Therefore, the experimental data reveals that the multilayer adsorption process occurs on the heterogeneous surface. In the Freundlich model, $1/n$ value demonstrates the strength of adsorption. If $n = 1$

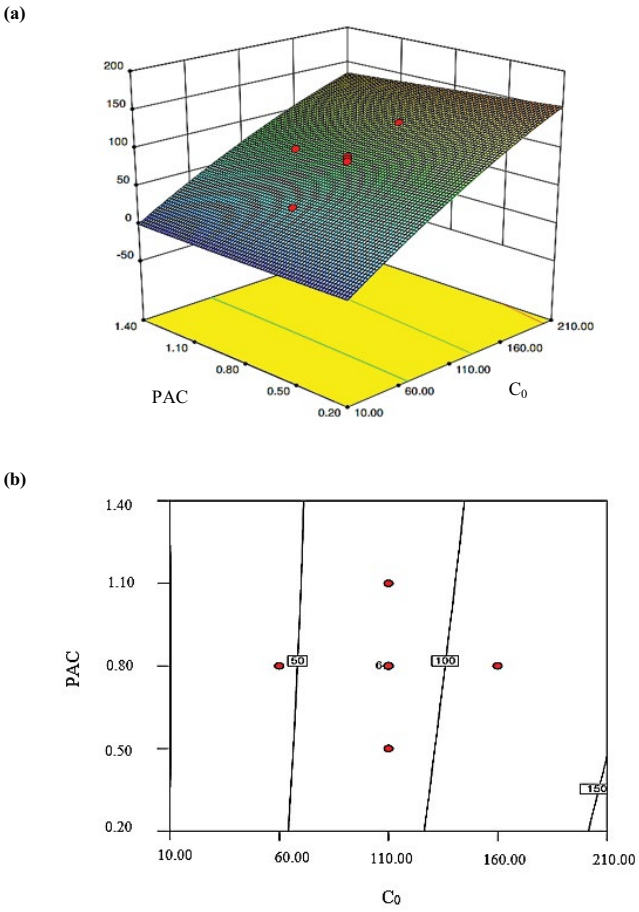

Fig. 6. (a) Three-dimensional (3D) and (b) two-dimensional response surface plots correlation between initial concentration of MB and PAC dosage on the MB removal (reaction time equal 30 min and pH equal 7).

indicates the linear adsorption, $n < 1$ implies chemical adsorption and $n > 1$ shows favorable physical adsorption [45,46]. From Table 4, n value equal to 0.33 corresponding to $1/n > 1$ which confirmed cooperative chemical adsorption.

The kinetic study of MB adsorption on the corn stalk activated carbon is studied and results are indicated in Table 5 and Figs. 8a and b. As observed, the pseudo-second-order model with higher R^2 (0.9833) compared to the pseudo-first-order model (R^2 = 0.8759) has a good fit with experimental data. The adsorption rate constant (K_2) is 0.018 min^{-1}. A comparison of adsorption rate constant (K_1 and K_2) for MB using different adsorbents which are previously reported, was performed and presented in Table 6. As a result, the prepared activated carbon showed a better adsorption rate in comparison to other adsorbents listed here.

3.4. Reusability result

The reusability of the prepared activated carbon was also studied by repeating the same experiment at optimum conditions (MB concentration of 10 mg L^{-1}, the adsorbent concentration of 1.4 g L^{-1} and pH of 11 after 10 min).

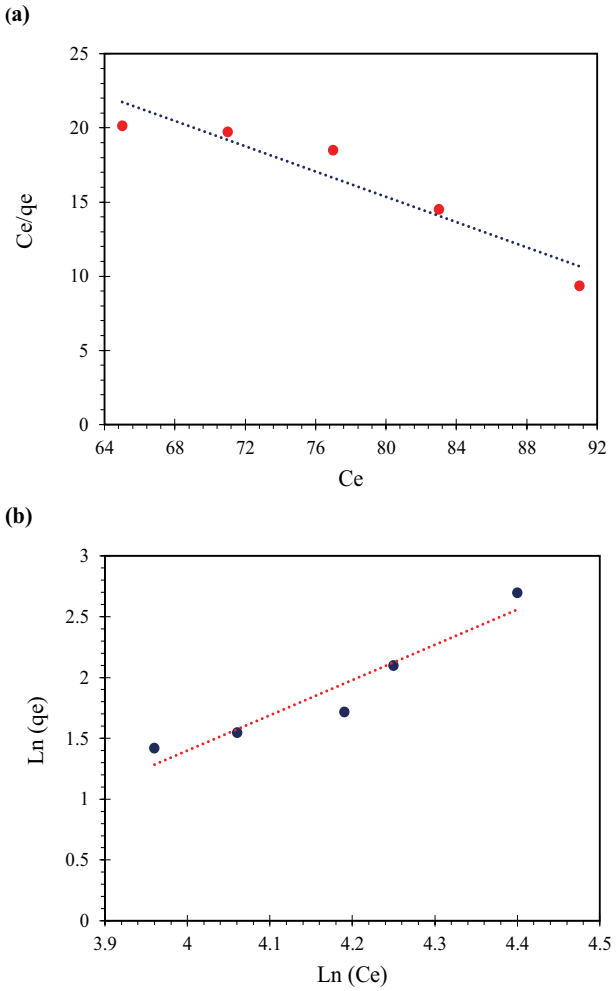

Fig. 7. (a) Langmuir and (b) Freundlich isotherm for MB adsorption on corn stalk activated carbon.

Table 4
Isotherm parameters for adsorption of MB onto the corn stalk activated carbon

Langmuir model	Freundlich model
$y = -0.426x + 49.434$	$y = 2.8971x - 10.189$
$R^2 = 0.90$	$R^2 = 0.91$
$K_L = 0.0086$ (L mg^{-1})	$K_F = 0.00004$ (mg$^{1-1/n}$ L$^{1/n}$ g^{-1})
$q_m = 2.347$ mg g^{-1}	$n = 0.345$

After the first cycle, the suspension of activated carbon and treated dye solution was centrifuged and activated carbon washed with deionized water. Finally, the activated carbon was dried at 110°C (3 h). The reusability of the prepared corn stalk activated carbon was proved when 75% removal efficiency could be achieved after 1 consecutive batch. The reusability result was confirmed by the FTIR spectrum which shows no obvious changes in the FTIR spectrum of regenerated activated carbon.

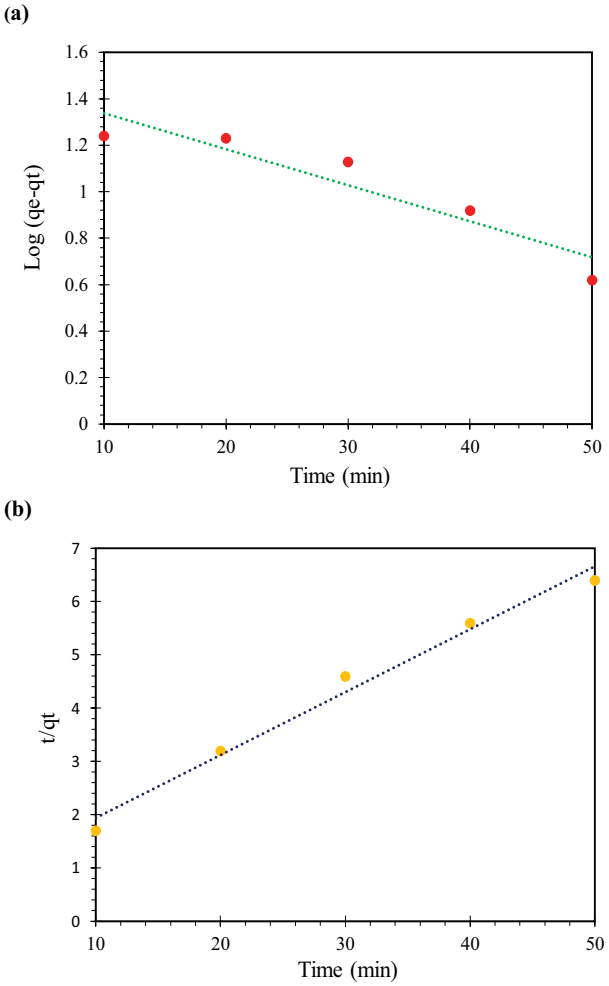

Fig. 8. Kinetic plot for MB adsorption on corn stalk activated carbon (a) pseudo-first-order model and (b) pseudo-second-order models.

Table 5
Kinetics models for MB adsorption onto the corn stalk activated carbon

Kinetic parameters	Pseudo-first-order kinetic model	Pseudo-second-order kinetic model
Equation	$y = -0.0155x + 1.493$	$y = 0.118x + 0.76$
R^2	0.8759	0.9833
Rate constant (min^{-1})	$K_1 = 0.0358$ (min^{-1})	$K_2 = 0.018$ (g mg^{-1} min^{-1})
q_e (mg g^{-1})	31.12	8.47

Table 6
Adsorption rate constant for MB dye by some other adsorbents reported in the literature

Sorbent	K_1 (min^{-1})	K_2 (g mg^{-1} min^{-1})	Kinetic models	C_0 (mg L^{-1})	References
Magnetic metal–organic frameworks (MOFs) (Fe_3O_4@AMCA-MIL-53(Al))	0.022	7.5×10^{-4}	Second-order	100	[47]
Brown macroalgae	0.032	0.003	Second-order	100	[48]
Magnetite/silica/pectin hybrid	0.0321	0.0028	Second-order	100	[49]
Magnetic 3-aminopropyltriethoxysilane	0.0148	0.0084	Second-order	20	[50]
Magnetite nanoparticles loaded tea waste	0.1726	0.0121	Second-order	20	[51]
Graphene/Fe_3O_4 composite	0.0574	0.2665	Second-order	25	[52]
Montmorillonite clay modified with iron oxide	0.014	0.0044	Second-order	100	[53]
This work	0.0358	0.018	Second-order	210	–

K_1: adsorption rate constant of a pseudo-first-order kinetic model
K_2: adsorption rate constant of a pseudo-second-order kinetic model

4. Conclusions

In this study, corn stalk was applied to synthesize activated carbon for the removal of MB from aqueous solution using batch sorption technique. The CCD was used to investigate the effect of initial MB concentration and adsorbent dosage, pH, and contact time, and the adsorption capacity of activated carbon was calculated as a response. The optimal condition was found at an initial concentration of 10 mg L^{-1} adsorbent dosage of 1.4 g pH of 11 and contact time 50 min with higher than 99.5% of MB removal. The adsorption parameters for the Langmuir and Freundlich isotherm models were determined and the equilibrium data were best fitted into the Freundlich isotherm model with acceptable $R^2 = 0.91$. The pseudo-second-order equation was best fitted for the kinetics of the MB adsorption process due to its high R^2.

Acknowledgment

The authors gratefully acknowledge the Research Council of Kermanshah University of Medical Sciences for financial support.

Symbols

C_0 — Initial concentration of dye solution, mg L^{-1}
q_e — Equilibrium adsorption capacity, mg g^{-1}
C_e — Dye concentration, mg L^{-1} at equilibrium
V — Volume of solution, L
W — Weight of adsorbent, g
q_m — Maximum adsorption capacity reflected a complete monolayer (mg g^{-1}) in Langmuir isotherm model
K_2 — Rate constant of pseudo-second-order adsorption, g mg^{-1} min^{-1}
K_1 — Equilibrium rate constant of pseudo-first-order adsorption, gg^{-1} min^{-1}
K_F — Isotherm constant indicates the capacity parameter (mg g^{-1}) related to the intensity of the adsorption
R^2 — Correlation coefficient
%R — Percentage of absorption process efficiency
β_0 — Offset term
β_{ij} — Interaction effect
β_{ii} — Squared effect
β_i — Linear effect
K_L — Langmuir constant or adsorption equilibrium constant (L mg^{-1}) that is related to the apparent energy of sorption
Y — Predicted response
n — Freundlich constant

References

[1] M.A. ul Hassan Rashid, M.M. Manzoor, S. Mukhtar, Urbanization and its effects on water resources: an exploratory analysis, Asian J. Water Environ. Pollut., 15 (2018) 67–74.
[2] S. Mousavi, S. Ibrahim, M.K. Aroua, Effects of operational parameters on the treatment of nitrate-rich wastewater by autohydrogenotrophic denitrifying bacteria, Water Environ. J., 28 (2014) 556–565.
[3] S.A. Mousavi, S. Ibrahim, Application of response surface methodology (RSM) for analyzing and modeling of nitrification process using sequencing batch reactors, Desal. Water Treat., 57 (2016) 5730–5739.
[4] P. Mohammadi, S. Ibrahim, M.S.M. Annuar, M. Khashij, S.A. Mousavi, A.A. Zinatizadeh, Optimization of fermentative hydrogen production from palm oil mill effluent in an up-flow anaerobic sludge blanket fixed film bioreactor, Sustainable Environ. Res., 27 (2017) 238–244.
[5] M. Mehralian, S.A. Mousavi, M.M. Mohamadreza, M. Khashij, Removal of Fe^{2+} from aqueous solution using manganese oxide coated zeolite and iron oxide coated zeolite, Int. J. Eng. Trans. B, 29 (2016) 1587.
[6] H. Zangeneh, A.A.L. Zinatizadeh, M. Habibi, M. Akia, M.H. Isa, Photocatalytic oxidation of organic dyes and pollutants in wastewater using different modified titanium dioxides: a comparative review, J. Ind. Eng. Chem., 26 (2015) 1–36.
[7] S.A. Mousavi, S. Nazari, Applying response surface methodology to optimize the Fenton oxidation process in the removal of Reactive Red 2, Pol. J. Environ. Stud., 26 (2017) 765–772.
[8] A.E. Pirbazari, E. Saberikhah, M. Badrouh, M.S. Emami, Alkali treated Foumanat tea waste as an efficient adsorbent for methylene blue adsorption from aqueous solution, Water Resour. Ind., 6 (2014) 64–80.
[9] S. Sadri Moghaddam, M.R. Alavi Moghaddam, M. Arami, Coagulation/flocculation process for dye removal using sludge from water treatment plant: optimization through response surface methodology, J. Hazard. Mater., 175 (2010) 651–657.
[10] M.Z.B. Mukhlish, M.M.R. Khan, A.R. Islam, A.N.M.S. Akanda, Removal of reactive dye from aqueous solution using coagulation–flocculation coupled with adsorption on papaya leaf, J. Mech. Eng. Sci., 10 (2016) 1884–1894.

[11] L. Gnanasekaran, R. Hemamalini, Mu. Naushad, Efficient photocatalytic degradation of toxic dyes using nanostructured TiO_2/polyaniline nanocomposite, Desal. Water Treat., 108 (2018) 322–328.
[12] D. Pathania, D. Gupta, A.H. Al-Muhtaseb, G. Sharma, A. Kumar, Mu. Naushad, T. Ahamad, S.M. Alshehr, Photocatalytic degradation of highly toxic dyes using chitosan-g-poly(acrylamide)/ZnS in presence of solar irradiation, J. Photochem. Photobiol., A, 329 (2016) 61–68.
[13] A. Kumar, G. Sharma, Mu. Naushad, P. Singh, S. Kalia, Polyacrylamide/$Ni_{0.02}Zn_{0.98}O$ nanocomposite with high solar light photocatalytic activity and efficient adsorption capacity for toxic dye removal, Ind. Eng. Chem. Res., 53 (2014) 15538–15548.
[14] S. Zinadini, A.A. Zinatizadeh, M. Rahimi, V. Vatanpour, H. Zangeneh, M. Beygzadeh, Novel high flux antifouling nanofiltration membranes for dye removal containing carboxymethyl chitosan coated Fe_3O_4 nanoparticles, Desalination, 349 (2014) 145–154.
[15] A. Almasi, Z. Rostamkhani, S.A. Mousavi, Adsorption of Reactive Red 2 using activated carbon prepared from walnut shell: batch and fixed bed studies, Desal. Water Treat. 79 (2017) 356–367.
[16] F. Silva, L. Nascimento, M. Brito, K. da Silva, W. Paschoal Jr., R. Fujiyama, Biosorption of Methylene Blue dye using natural biosorbents made from weeds, Materials, 12 (2019) 2486–2498.
[17] R. Vital Kandisa, N. Saibaba, K. Beebi Shaik, R. Gopinath, Dye removal by adsorption: a review, Biorem. Biodegrad., 7 (2016) 371, doi: 10.4172/2155-6199.1000371.
[18] G. Sharma, Mu. Naushad, A. Kumar, S. Rana, S. Sharma, A. Bhatnagar, F.J. Stadler, A.A. Ghfar, M. Rizwan Khan, Efficient removal of coomassie brilliant blue R-250 dye using starch/poly(alginic acid-*cl*-acrylamide) nanohydrogel, Process Saf. Environ., 109 (2017) 301–310.
[19] S. Rattanapan, J. Srikram, P. Kongsune, Adsorption of Methyl Orange on coffee grounds activated carbon, Energy Procedia, 138 (2017) 949–954.
[20] Y.H. Cao, K.L. Wang, X.M. Wang, Z.R. Gu, T. Ambrico, W. Gibbons, Q.H. Fan, A.-A. Talukder, Preparation of active carbons from corn stalk for butanol vapor adsorption, J. Energy Chem., 26 (2017) 35–41.
[21] J.K. Ratan, M. Kaur, B. Adiraju, Synthesis of activated carbon from agricultural waste using a simple method: characterization, parametric and isotherms study, Mater. Today Proc., 5 (2018) 3334–3345.
[22] S.H. Chen, Q.Y. Yue, B.Y. Gao, Q. Li, X. Xu, K.F. Fu, Adsorption of hexavalent chromium from aqueous solution by modified corn stalk: a fixed-bed column study, Bioresour. Technol., 113 (2012) 114–120.
[23] S.H. Chen, Y. Zhu, Z.J. Han, G. Feng, Y.L. Jia, K.F. Fu, Q.Y. Yue, Adsorption of hexavalent chromium on modified corn stalk using different cross-linking agents, IOP Conf. Ser.: Mater. Sci. Eng., 274 (2017) 12–20.
[24] M. Husseien, A.A. Amer, A. El-Maghraby, N. Hamedallah, A comprehensive characterization of corn stalk and study of carbonized corn stalk in dye and gas oil sorption, J. Anal. Appl. Pyrolysis, 86 (2009) 360–363.
[25] L.B.L. Lim, N. Priyantha, D.T.B. Tennakoon, H.I. Chieng, M.K. Dahri, M. Suklueng, Breadnut peel as a highly effective low-cost biosorbent for methylene blue: equilibrium, thermodynamic and kinetic studies, Arabian J. Chem., 10 (2017) S3216–S3228.
[26] D. Nayeri, S.A. Mousavi, A. Mehrabi, Oxytetracycline removal from aqueous solutions using activated carbon prepared from corn stalks, *J. Appl. Res. Water Wastewater*, 6 (2019) 67–72.
[27] S. Jain, R.V. Jayaram, Removal of basic dyes from aqueous solution by low-cost adsorbent: wood apple shell (*Feronia acidissima*), Desalination, 250 (2010) 921–927.
[28] D. Balarak, J. Jaafari, G. Hassani, Y. Mahdavi, I. Tyagi, S. Agarwal, V.K. Gupta, The use of low-cost adsorbent (Canola residues) for the adsorption of methylene blue from aqueous solution: isotherm, kinetic and thermodynamic studies, Colloid Interface Sci. Commun., 7 (2015) 16–19.
[29] E.H. Ezechi, S.R. bin Mohamed Kutty, A. Malakahmad, M.H. Isa, Characterization and optimization of effluent dye removal using a new low-cost adsorbent: equilibrium, kinetics and thermodynamic study, Process Saf. Environ. Prot., 98 (2015) 16–32.
[30] D. Shahbazi, S.A. Mousavi, D. Nayeri, Low-cost activated carbon: characterization, decolorization, modeling, optimization and kinetics, Int. J. Environ. Sci. Technol., (2020), https://doi.org/10.1007/s13762–020–02698-w.
[31] B. Kamarehie, E. Aghaali, S.A. Mousavi, S.Y. Hashemi, A. Jafari, Nitrate removal from aqueous solutions using granular activated carbon modified with iron nanoparticles, Int. J. Eng. Trans. A, 31 (2018) 554–563.
[32] Mu. Naushad, S. Vasudevan, G. Sharma, A. Kumar, Z.A. ALOthman, Adsorption kinetics, isotherms, and thermodynamic studies for Hg^{2+} adsorption from aqueous medium using alizarin red-S-loaded amberlite IRA-400 resin, Desal. Water Treat., 57 (2016) 18551–18559.
[33] Mu. Naushad, Z.A. ALOthman, R. Awual, S.M. Alfadul, T. Ahamad, Adsorption of rose Bengal dye from aqueous solution by amberlite Ira-938 resin: kinetics, isotherms, and thermodynamic studies, Desal. Water Treat., 57 (2016) 13527–13533.
[34] X. Chen, Modeling of experimental adsorption isotherm data, Information, 6 (2015) 14–22.
[35] K.S. Padmavathy, G. Madhu, P.V. Haseena, A study on effects of pH, adsorbent dosage, time, initial concentration and adsorption isotherm study for the removal of hexavalent chromium (Cr(VI)) from wastewater by magnetite nanoparticles, Procedia Technol., 24 (2016) 585–594.
[36] H.S. Shang, Y.J. Lu, F. Zhao, C. Chao, B. Zhang, H. Zhang, Preparing high surface area porous carbon from biomass by carbonization in a molten salt medium, RSC Adv., 5 (2015) 75728–75734.
[37] M.S. Islam, B.C. Ang, S. Gharehkhani, A.B.M. Afifi, Adsorption capability of activated carbon synthesized from coconut shell, Carbon Lett., 20 (2016) 1–9.
[38] S.A. Mousavi, M. Mehralian, M. Khashij, S. Parvaneh, Methylene Blue removal from aqueous solutions by activated carbon prepared from *N. microphyllum* (AC-NM): RSM analysis, isotherms and kinetic studies, Global NEST J., 19 (2017) 697–705.
[39] J.R. Kim, B. Santiano, H.S. Kim, E.S. Kan, Heterogeneous oxidation of Methylene Blue with surface-modified iron-amended activated carbon, Am. J. Anal. Chem., 4 (2013) 115–122.
[40] E.N. El Qada, S.J. Allen, G.M. Walker, Adsorption of basic dyes from aqueous solution onto activated carbons, Chem. Eng. J., 135 (2008) 174–184.
[41] S.B. Wang, Z.H. Zhu, A. Coomes, F. Haghseresht, G.Q. Lu, The physical and surface chemical characteristics of activated carbons and the adsorption of Methylene Blue from wastewater, J. Colloid Interface Sci., 284 (2005) 440–446.
[42] T. Teka, S. Enyew, Study on effect of different parameters on adsorption efficiency of low cost activated carbon for the removal of methylene blue dye, Int. J. Innovative Sci. Res., 8 (2014) 106–111.
[43] M. Mulugeta, B. Lelisa, Removal of Methylene Blue (Mb) dye from aqueous solution by bioadsorption onto untreated *Parthenium hystrophorous* weed, Mod. Chem. Appl., 2 (2014) 2–5.
[44] M. Khairud Dahri, M. Raziq Rahimi Kooh, L.B.L. Lim, Application of *Casuarina equisetifolia* needle for the removal of methylene blue and malachite green dyes from aqueous solution, Alexandria Eng. J., 54 (2015) 1253–1263.
[45] A.M. Aljeboree, A.N. Alshirifi, A.F. Alkaim, Kinetics and equilibrium study for the adsorption of textile dyes on coconut shell activated carbon, Arabian J. Chem., 10 (2017) S3381–S3393.
[46] Z.A. AL-Othman, R. Ali, Mu. Naushad, Hexavalent chromium removal from aqueous medium by activated carbon prepared from peanut shell: adsorption kinetics, equilibrium and thermodynamic studies, Chem. Eng. J., 184 (2012) 238–247.
[47] A.A. Alqadami, Mu. Naushad, Z.A. ALOthman, T. Ahamad, Adsorptive performance of MOF nanocomposite for methylene

blue and malachite green dyes: kinetics, isotherm and mechanism, J. Environ. Manage., 223 (2018) 29–36.
[48] E. Daneshvar, A. Vazirzadeh, A. Niazi, M. Kousha, Mu. Naushad, A. Bhatnagar, Desorption of Methylene blue dye from brown macroalga: effects of operating parameters, isotherm study and kinetic modeling, J. Cleaner Prod., 152 (2017) 443e453.
[49] O.A. Attallah, M.A. Al-Ghobashy, M. Nebsen, M.Y. Salem, Removal of cationic and anionic dyes from aqueous solution with magnetite/pectin and magnetite/silica/pectin hybrid nanocomposites: kinetic, isotherm and mechanism analysis, RSC Adv., 6 (2016) 11461–11480.
[50] F. Ge, H. Ye, M.-M. Li, B.-X. Zhao, Efficient removal of cationic dyes from aqueous solution by polymer-modified magnetic nanoparticles, Chem. Eng. J., 198–199 (2012) 11–17.
[51] T. Madrakian, A. Afkhami, M. Ahmadi, Adsorption and kinetic studies of seven different organic dyes onto magnetite nanoparticles loaded tea waste and removal of them from wastewater samples, Spectrochim. Acta, Part A, 99 (2012) 102–109.
[52] L.H. Ai, C.Y. Zhang, Z.L. Chen, Removal of methylene blue from aqueous solution by a solvothermal-synthesized graphene/magnetite composite, J. Hazard. Mater., 192 (2011) 1515–1524.
[53] L. Cottet, C.A.P. Almeida, N. Naidek, M.F. Viante, M.C. Lopes, N.A. Debacher, Adsorption characteristics of montmorillonite clay modified with iron oxide with respect to methylene blue in aqueous media, Appl. Clay Sci., 95 (2014) 25–31.